Screening of Aqueous Amine-Based Solvents for Postcombustion CO2 Capture by Chemical Absorption

ARTICLE *in* CHEMICAL ENGINEERING & TECHNOLOGY · MARCH 2012

Impact Factor: 2.44 · DOI: 10.1002/ceat.201100523

2 AUTHORS:

Lionel Dubois
Université de Mons
9 PUBLICATIONS **81** CITATIONS
SEE PROFILE

Diane Thomas
Université de Mons
49 PUBLICATIONS **507** CITATIONS
SEE PROFILE

Lionel Dubois

Diane Thomas

University of Mons, Faculty of Engineering, Chemical Engineering Department, Mons, Belgium.

Research Article

Screening of Aqueous Amine-Based Solvents for Postcombustion CO_2 Capture by Chemical Absorption

In relation with CO_2 capture by chemical absorption into aqueous amine-based solvents, absorption and regeneration parameters by separate absorption and regeneration tests are determined. An absorption parameter for different types of amine-based solvents is evaluated by performing absorption tests at 298 K and atmospheric pressure with a gas-liquid contactor and deducing apparent kinetic constants. The regeneration parameter is obtained from a CO_2 concentration temporal profile measured in a regeneration cell at the boiling temperature of each solvent. By combining both parameters it is possible to compare the absorption-regeneration performances of all the solvents studied. Good absorption-regeneration performances of cyclical amines, especially of piperidine (PIP) and piperazine (PZ), are highlighted. The interesting potential of 2-amino-2-methyl-1-propanol (AMP) and methyldiethanolamine (MDEA) activated with PZ and PIP is also considered.

Keywords: Absorption parameter, Amines, Carbon dioxide capture, Regeneration parameter

Received: October 03, 2011, *revised:* December 02, 2011; *accepted:* December 19, 2011

DOI: 10.1002/ceat.201100523

1 Introduction

The reduction of CO_2 emissions as the main source for anthropogenic greenhouse effects requires implementation of environmental solutions such as oxycombustion [1], precombustion [2], or postcombustion [3] CO_2 capture. This work focuses on the third technology, especially on the CO_2 absorption process into amine-based solvents which combines two steps: (i) absorption of CO_2 by countercurrent contact between gas and solvent in the absorption column, and (ii) regeneration of the solvent in a second column by heating supply releasing a concentrated CO_2 flux.

The use of an alkanolamine-based solution such as monoethanolamine (MEA) remains the preferred choice for such a gas treating technology, but alternative solvents more competitive than MEA are required taking different aspects into account, such as absorption performances and energy consumption for solvent regeneration, solvent resistance to degradation [4, 5] (which can induce corrosion problems [6, 7] and higher solvent consumption), solvent toxicity [8], and volatility [9]. Among these, absorption and regeneration efficiencies were found to be the two most important criteria in solvent screening, as discussed, e.g., in technical and economic studies [10, 11].

The following amine solutions (chemical structures in Fig. 1) were tested: monoethanolamine (MEA), a primary alkanolamine which is considered as benchmark in most studies; *N*-methyldiethanolamine (MDEA), a tertiary alkanolamine; 2-amino-2-methyl-1-propanol (AMP), a sterically hindered amine (SHA), and three cyclical amines usually applied as absorption activators, namely piperidine (PIP), a cyclical monoamine, piperazine (PZ), a cyclical diamine, and piperazinyl-1,2-ethylamine (PZEA), a cyclical triamine with the particularity of containing three amine functions (primary, secondary, and tertiary).

Modeling of the absorption process using aqueous amine solutions and deduction of characteristic solvent parameters require the knowledge of CO_2 absorption-reaction mechanisms taking place for the different types of amine solutions. The various reaction mechanisms (zwitterion, termolecular, and base-catalyzed hydration) as well as data on reaction kinetics of individual amine systems and their mixtures or innovative amine-based solvents have been extensively reviewed [12, 13] and only a brief summary is here presented.

The reaction mechanisms generally considered for CO_2 absorption with primary amines (R_1–NH_2 with $R_1 = (CH_2)_2$–OH for MEA) or secondary amines (R_1R_2–NH) is the formation of a zwitterion intermediate leading to carbamate formation [14, 15]:

Correspondence: Prof. D. Thomas (Diane.Thomas@umons.ac.be), University of Mons, Faculty of Engineering, Chemical Engineering Department, 7000 Mons, Belgium.

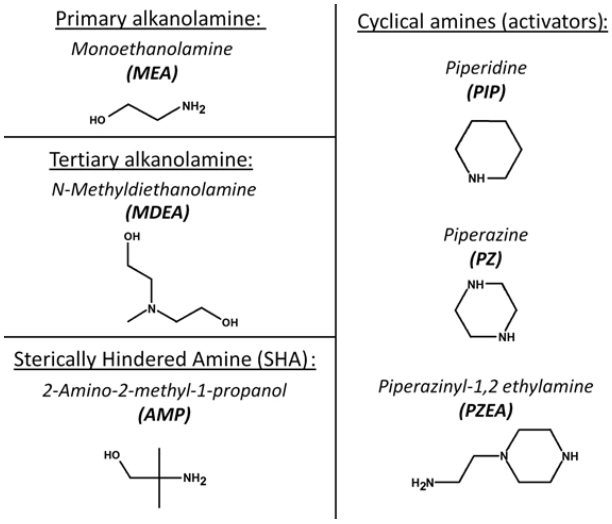

Figure 1. Studied amines.

$$CO_2 + R_1R_2\text{–}NH \rightleftharpoons R_1R_2\text{–}NH^+COO^- \quad (1)$$

$$R_1R_2\text{–}NH^+COO^- + B \rightleftharpoons R_1R_2\text{–}NCOO^- + BH^+ \quad (2)$$

where B is a basic compound which can be an amine, OH^-, or H_2O.

Due to the strong heat of absorption associated with carbamate formation, the regeneration costs of these amines are substantial [16, 17].

Sterically hindered amines such as AMP are characterized by the fact that due to the hindrance of the bulky group adjacent to the amino group, the formed carbamate is very unstable and a hydrolytic reaction takes place, subsequently leading to bicarbonate formation as ultimate product of the reaction. Therefore, this class of amines leads to lower regeneration costs than classical primary and secondary amines. The application of SHA in gas treating technology offers also advantages [18] in comparison with conventional amines for CO_2 removal from gases [19], such as higher absorption capacity, selectivity, and degradation resistance.

For tertiary alkanolamines ($R_1R_2R_3$–N with $R_1 = CH_3$ and R_2, $R_3 = (CH_2)_2$–OH for MDEA), the absence of a hydrogen atom attached to the nitrogen atom leads to the formation of a bicarbonate [13]:

$$CO_2 + H_2O \rightleftharpoons H^+ + HCO_3^- \quad (3)$$

$$R_1R_2R_3\text{–}N + H^+ \rightleftharpoons R_1R_2R_3\text{–}NH^+ \quad (4)$$

with the overall reaction:

$$CO_2 + R_1R_2R_3\text{–}N + H_2O \rightleftharpoons R_1R_2R_3\text{–}NH^+ + HCO_3^- \quad (5)$$

Even if the reactivity of this amine with CO_2 is quite low as the carbamate formation reaction cannot take place, the lower reaction heat released with bicarbonate formation than with carbamate formation results in reduced solvent regeneration costs with the tertiary amines [16].

To improve the CO_2 absorption rates of tertiary amines, small amounts of absorption activators (cyclical amines in most cases) can be added to the tertiary amines in order to reach sufficient absorption performances (as, e.g., in [20] and [21] for activation of MDEA with PZ), the absorption capacities of the solutions remaining high.

Considering the different behaviors of the various amine types, here the absorption-regeneration performances of different aqueous amine-based solvents, single or blended with absorption activators, were evaluated. In literature, less information is available on blended solvents. Separate absorption and regeneration tests were carried out in order to deduce relevant characteristics and compare the absorption-regeneration performances of the solvents. As already described in previous works [22, 23], the intention of such a research is to present the absorption and regeneration performances of a solvent on a global graph, comparing easily the solvents under both aspects, and to define adequately the parameters which characterize absorption and regeneration phases.

Regarding the absorption phase, the CO_2 absorption flux is directly proportional to the product of the kinetic constant and the amine concentration, defined as the apparent kinetic constant k_{app}. This can give a good idea of the absorption performances of the solvent. The regeneration phase, especially the regeneration energy (E_{regen}), includes three contributions:

$$E_{regen} = \Delta H_{reaction} + \Delta H_{sensible} + \Delta H_{vaporization} \quad (6)$$

where $\Delta H_{reaction}$ is the energy used to reverse the reaction taking place during absorption, $\Delta H_{sensible}$ is the sensible heat required to reach the regeneration temperature, and $\Delta H_{vaporization}$ is the energy necessary to vaporize the solvent (composed of water and amine(s)). Considering $\Delta H_{reaction}$ as unique indicator of the regeneration energy (as in [22, 23]) would give a wrong idea of the regeneration performances because even if $\Delta H_{reaction}$ is generally the major part of E_{regen}, the other terms can really differ from one amine type to another [24]. Therefore, the regeneration parameter defined in this work is based on a desorption kinetic constant obtained from regeneration efficiency measurements. Such an indicator is consequently influenced by all three contributions of E_{regen}. Finally, the challenge of this research is to find solvents (singles or blends) presenting simultaneously an absorption parameter as high as possible and a regeneration parameter as low as possible.

2 Experimental

2.1 Gas and Liquid Analysis

The necessary analysis of the CO_2 content in the gas phase was performed with an infrared analyzer (Emerson, model X-STREAM X2GP, three-way measurement in the ranges of 0–20 % or 0–100 %). The sampling lines were designed to avoid the presence of water in the analyzer by adding permeation dryers (Perma Pure, model MD 110 24 PP). This type of dryer is composed of a membrane made of Nafion (copolymer of Teflon) creating an exchange area between the sample gas

and a drying gas (nitrogen in our case), thus allowing moisture to be transferred through the membrane. The analysis of the CO_2 content in the liquid phase was performed by total carbon analysis by means of a TOC analyzer (Shimadzu, model TOC-VCSH, NDIR detector, calibrated in the range of 0–1000 mg C/L with a standardized solution of potassium hydrogen phthalate). The CO_2 loading of the solvents was determined by the difference between the total carbon contents of loaded and unloaded solutions. The pH of the solution was measured with a pH meter (Mettler Toledo, model FiveGo FG2-Basic, electrode LE438 in polypropylene).

2.2 Absorption Tests

The experimental equipment used for the absorption tests (Fig. 2), including a cable-bundle scrubber, liquid and gas supplies, and a gas sampling part, together with the experimental procedure and conditions (see Tab. 1) are described more detailed in [25, 26].

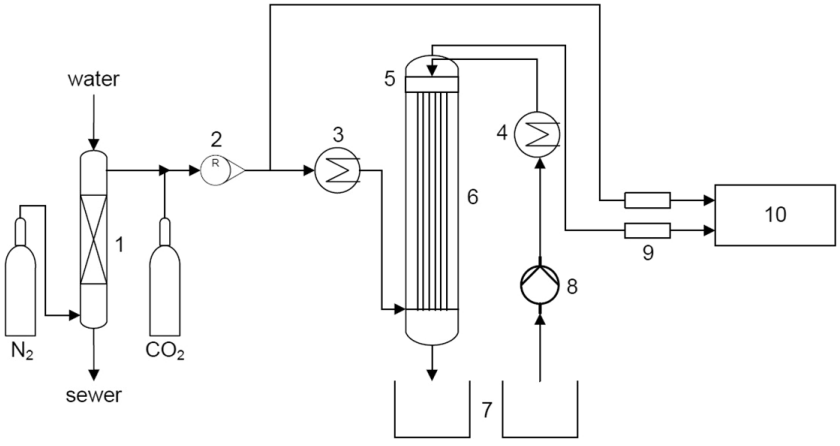

Figure 2. Experimental apparatus for the absorption tests including the gas-liquid contactor: (1) humidification column, (2) flow indicator/control, (3), (4) heat exchangers, (5) liquid distributor, (6) cable-bundle contactor, (7) solution tanks, (8) liquid pump, (9) membrane dryers, (10) gas analysis.

Table 1. Operating conditions of the absorption tests.

Pressure (P)	101.325 kPa		
Temperature (T)	298.15 K		
Liquid flow rate (L)	$3.18 \cdot 10^{-6}\ m^3 s^{-1}$		
Gas flow rate (G)	$2.25 \cdot 10^{-4}\ m^3 s^{-1}$		
CO_2 contents ($y_{CO_2,in}$)	4–18 %		
Amine-based solvents	Amine	Type	Concentration (c_{Amine})
	AMP	Sterically hindered	15–45 wt-%
	MEA	Primary	5–30 wt-%
	PZ	Cyclical	5–12.5 wt-%
	PZEA	Cyclical	5–10 wt-%
	MDEA	Tertiary	30–50 wt-%

The amine-based absorbent was fed to the top distributing chamber by means of a peristaltic pump and distributed on all the vertical yarns contacting the gas continuously and countercurrently. The gas phase was composed of nitrogen humidified in a saturator (packed column fed with water), in which CO_2 was added to obtain the desired concentration (4–18 vol.-%). The total gas flow rate was metered by a rotameter. Sampling of gas simultaneously at the input and output of the column was performed continuously through membrane dryers followed by an IR analyzer, giving the molar fractions $y_{CO2,in}$ and $y_{CO2,\ out}$, which allowed calculating the CO_2 absorption efficiency (A) for different scrubbing solutions:

$$A = \frac{G_{in} y_{CO_2,in} - G_{out} y_{CO_2,out}}{G_{in} y_{CO_2,in}} \quad (7)$$

where G_{in} and $y_{CO_2,in}$ are the gas flow rate and CO_2 volume fraction in the gas phase at the inlet of the contactor, and G_{out} and $y_{CO_2,out}$ are the gas flow rate and CO_2 volume fraction in the gas phase at the outlet of the contactor.

All experiments reported here were carried out under atmospheric pressure and at a temperature of 298 K. Hydrodynamic conditions, namely gas and liquid flow rates, were kept constant in all the experiments, comparing only different amine solvents. The superficial gas velocity was maintained at $0.17\ m\ s^{-1}$. The liquid flow rate was fixed to $32\ cm^3 min^{-1}$ per cable for the cable contactor (total flow rate: $11.5\ L\ h^{-1}$), which is the nominal value for this kind of cable scrubber.

2.3 Regeneration Tests

The regeneration device is presented in Fig. 3. It is composed of a three-necked flask of 0.25 L, a thermo-regulated heating system (Ika, model RCT Basic, maximum heating power of 600 W) with a Pt100 temperature sensor immersed in the solution, and a magnetic stirring system (maximum stirring speed of 1500 rpm). A condenser installed at the top of the flask and flowed by cooling water provided by an external cooling system (Huber, model Minichiller) aimed at condensing the vapor products issued from the evaporation of the aqueous CO_2-amine solutions.

The operating conditions of the regeneration tests are summarized in Tab. 2. The total amine concentration of the solvent was fixed at 30 wt-% except for PZ and PIP (15 wt-%) due to a solubility limit.

Prior to the regeneration test, the carbon content of the unloaded amine solution was measured with the TOC analyzer. Using a gas bubbler with a pure CO_2 flow

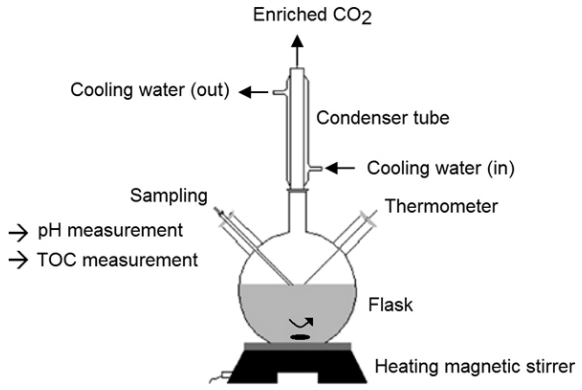

Figure 3. Experimental apparatus with regeneration device.

Table 2. Operating conditions of the regeneration tests.

Heating power	600 W
Liquid volume	0.2 L
Liquid agitation speed	35 rpm
Condenser length	0.35 m
Condenser water temperature (from thermostated bath)	278 K
Regeneration time	7200 s
Total amine concentration	15 and 30 wt-%

rate of 10 L min^{-1} during 40 min, 300 mL of amine(s) solution was gradually loaded with CO_2 up to its saturation. This step was followed by nitrogen bubbling with a flow rate of 10 L min^{-1} during 20 min in order to eliminate the physically dissolved CO_2. At the end of the saturation step, the loaded amine solution was analyzed using the TOC analyzer in order to determine its CO_2 concentration (C_{CO2} ($t = 0$)) and calculate its CO_2 loading (a_{CO_2} ($t = 0$)) according to:

$$a_{CO_2}(t=0) = \frac{C_{CO_2}(t=0)}{C_{amine}} \tag{8}$$

where C_{amine} is the total amine concentration of the solvent. The solution was then transferred into the regeneration cell where it was stirred and heated with a fixed heating power up to its boiling point. The duration of the test was set to 120 min (see Tab. 2). During the test, samples of the solution are regularly withdrawn and analyzed to determine their pH (pH (t)) and their CO_2 loading (a_{CO2} (t)) allowing to deduce the regeneration efficiency (η_{regen} (t)) of the solution, conventionally defined as (see, e.g., [27], [28]):

$$\eta_{regen}(t) = \frac{a_{CO_2}(t=0) - a_{CO_2}(t)}{a_{CO_2}(t=0)} = \frac{\Delta a_{CO_2}}{a_{CO_2}(t=0)} \tag{9}$$

This regeneration efficiency has the advantage over the CO_2 cycling capacity (Δa_{CO_2}) that it is divided by the initial CO_2 loading of the solution. Actually, the starting point (a_{CO_2} ($t = 0$)) of a regeneration process influences the regeneration performances of a solvent for the same Δa_{CO_2} values.

Although such tests do not yield directly the regeneration energy, the screening of solvents that require low energy for the regeneration step is considered by the comparison of desorption kinetics measured for different solvents under identical operating conditions [27]. In addition, even if blended solutions of amines seem to have good capabilities for CO_2 capture due to the activation mechanism, such data are still rather limited in the case of amine mixtures.

3 Modeling of Absorption Performances

3.1 Theoretical Modeling Principles

A modeling method based on the two-film theory for CO_2 absorption accompanied by an irreversible chemical reaction between the solute (CO_2) and the liquid reactant (amine solution) was developed in order to simulate the CO_2 absorption performances of the amine solutions. The chemical reaction regime can be slow, moderately fast, or fast (Hatta number criteria [29]) depending on the liquid phase concentration and the kinetic constant CO_2-amine. The Hatta number is defined as:

$$\mathrm{Ha} = \frac{\sqrt{k_2 D_{CO_2/Amine}\, c_{Amine}}}{k_L} \tag{10}$$

where k_2 (m^{3}kmol^{-1}s^{-1}) is the kinetic constant of the CO_2 reaction with the amine, $D_{CO_2/Amine}$ (m^{2}s^{-1}) is the diffusion coefficient for CO_2 in the amine solution, c_{Amine} (kmol m^{-3}) is the molar concentration of the amine, and k_L (m s^{-1}) is the liquid-phase mass transfer coefficient.

Due to the rapid reaction which proceeds and consumes the solute, the CO_2 concentration in the liquid film is virtually zero ($c_{CO_2} = 0$) and the absorption flux R_{CO_2} (kmol m^{-2}s^{-1}) can be written as:

$$R_{CO_2} = k_G(p_{CO_2} - p_{CO_2,i}) = E\, k_L\, C_{CO_2,i} \tag{11}$$

where k_G (kmol m^{-2}s^{-1}Pa^{-1}) is the gas-phase mass transfer coefficient, p_{CO_2} (Pa) is the partial pressure of CO_2, and $p_{CO_2,i}$ (Pa) and $C_{CO_2,i}$ (kmol m^{-3}) are, respectively, the interfacial values of the CO_2 partial pressure and concentration assuming a Henry's equilibrium relation ($p_{CO_2,i} = H_{CO_2/Amine} c_{CO_2,i}$) at the gas-liquid interface with the Henry's coefficient $H_{CO_2/Amine}$ (Pa m^{3}kmol^{-1}). E (–) represents the enhancement factor.

For the present conditions of a high CO_2 reactivity with the amine and an amine concentration in the liquid bulk being much greater than the CO_2 interfacial concentration, thus leading to high Hatta numbers ($3 < \mathrm{Ha} < E_i/2$, with E_i being the value of E for the instantaneous reaction), the kinetic regime of the absorption-reaction process becomes pseudo-first order and fast. The enhancement factor E is almost equal to Ha [29] and Eq. (12) is used to compute the liquid side absorption flux (R_{CO_2}):

$$\begin{aligned} R_{CO_2} &= \frac{\sqrt{k_2\, D_{CO_2/Amine}}}{H_{CO_2/Amine}} \sqrt{c_{Amine}}\, p_{CO_2,i} \\ &= \frac{\sqrt{k_{app}\, D_{CO_2/Amine}}}{H_{CO_2/Amine}} p_{CO_2,i} \end{aligned} \tag{12}$$

where $k_{app} = k_2 c_{Amine}$ is defined as an apparent kinetic constant.

3.2 Computation of Performances for the Absorption Test Runs and Second-Order Kinetic Constant Determination

By means of a finite difference method, the column simulation was made considering small height incremental volumes (dh = 0.01 m), the molar fraction of CO_2 (y_{CO_2}), amine concentration (c_{Amine}), and absorption flux (R_{CO_2}) being centered in these elements. To compute the CO_2 partial pressure (molar fraction) and the amine concentration in the liquid along the column taking account of the operating fluid flow rates (L and G, values given in Tab. 1), classical steady-state mass balances were used:

$$R_{CO_2} aS\,dh = \frac{L}{n}(c_{Amine,I} - c_{Amine,O}) = \frac{PG}{RT}(y_{CO_2,I} - y_{CO_2,O}) \quad (13)$$

where I and O refer to the inlet and outlet of the incremental volume, a (m^{-1}) is the specific interfacial area, S (m^2) is the section of the contactor, and n corresponds to the stoichiometry of the global reaction CO_2/amine and is equal to 1 for MDEA, AMP, and PZEA, and equal to 2 for MEA and PZ.

Starting from the top of the contactor ($y_{CO_2,out}$ and $c_{Amine,in}$ are given), the program provides finally the CO_2 inlet molar fraction ($y_{CO_2,in}$) which is compared to the experimental value or in terms of absorption efficiencies (A). A schematic representation of this methodology is provided in Fig. 4.

This modeling method finally allowed to deduce second-order kinetic constants k_2 (at 298 K) from our absorption test runs [30] by minimizing (least squares method) the sum of the squared residuals defined as differences between experimental values and model values of the absorption efficiencies for the different amine concentrations experimented:

$$\min \sum_j (A_{exp,j} - A_{sim,j})^2 \quad (14)$$

The calculation method was validated in our previous work [28].

4 Experimental and Simulation Results: Determination of Absorption and Regeneration Parameters

4.1 Absorption Results and Simulations

The absorption results obtained with the cable-bundle contactor are compared in Fig. 5 in terms of CO_2 absorption efficiencies for single and blended amine solutions and for 15 vol.-% CO_2 content in the gas. Significant differences between absorption efficiencies of the different types of amine solutions are observed: very low for a tertiary amine (MDEA), better with a sterically hindered amine (AMP), and excellent with a primary amine (MEA) or with absorption activators (e.g., PZ). This general observation can be easily related to the kinetic characteristics of these amine solutions.

For CO_2 absorption into aqueous blended amine solutions and especially when a cyclical amine (PZ or PZEA) or a primary amine (MEA) is added to MDEA (30 wt-%) or AMP (30 wt-%) aqueous solutions, the CO_2 absorption rates can be substantially increased due to the activation phenomenon. The CO_2 absorption rate of MEA (30 wt-%) can also be increased with addition of PZ (5 wt-%). As illustrated in Fig. 6, the different absorption tests were satisfactorily simulated with our modeling method using the kinetic constants deduced. Moreover, these constants were successfully compared to literature

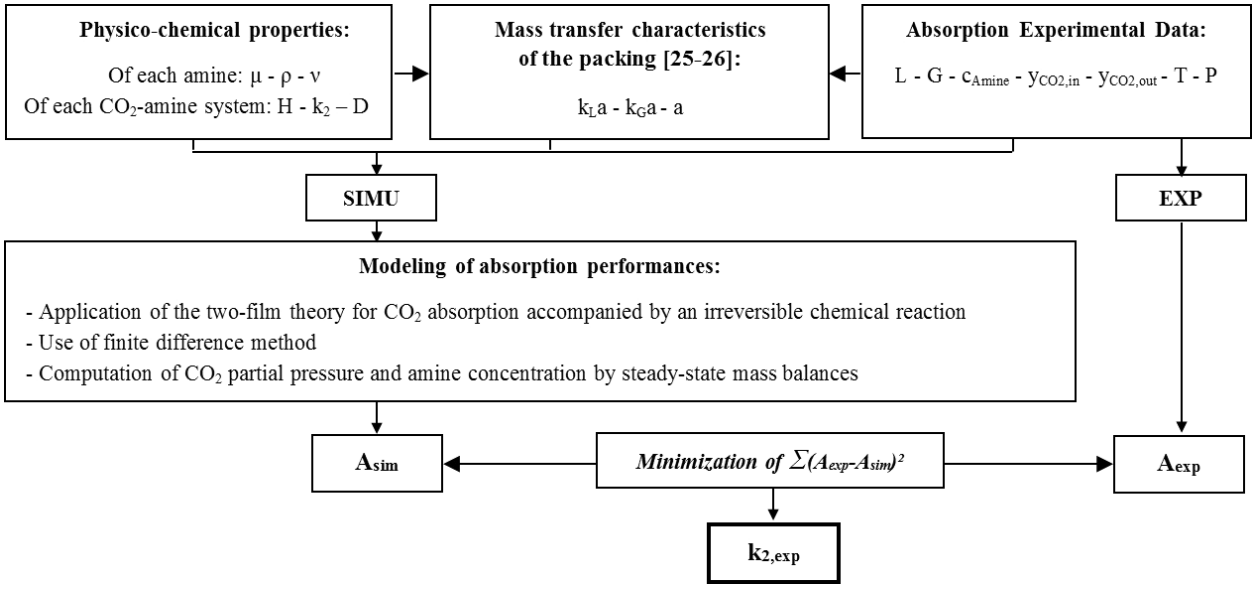

Figure 4. Methodology for modeling and kinetic constant determination.

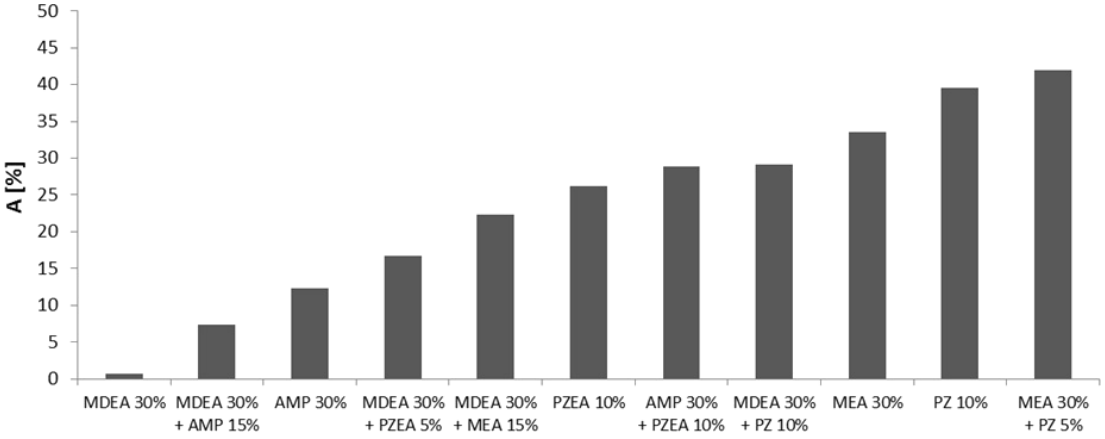

Figure 5. Absorption rate comparison for CO_2 content in the inlet gas (15 vol.-%).

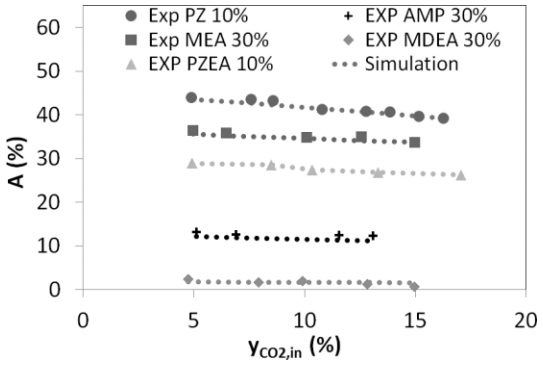

Figure 6. Comparison between experimental and simulated results (with $k_{2,exp}$).

values listed in Tab. 3. Fig. 6 indicates a slightly decreasing absorption efficiency as the CO_2 molar concentration in the gas phase is increased, due to an increased amine consumption which to some extent decelerates the absorption process.

Applying our experimental kinetic constants, except for PIP which was not experimented (kinetic data from [35]), it is possible to estimate apparent kinetic constants (k_{app}) as:

$$k_{app}\ (s^{-1}) = k_2 C_{amine} \text{ for a simple amine} \quad (15)$$

$$k_{app}(s^{-1}) = \sum_x k_{2,x} C_{amine,x} \quad (16)$$

for mixtures composed of x amines

The CO_2 absorption flux (R_{CO_2}) is directly proportional to k_{app}, as defined in Eq. (11).

For the case of amine blends, Eq. (16) was used successfully in [37] by considering that the reaction model can be regarded as two parallel rapid pseudo-first-order reactions relative to each CO_2-amine system.

Finally, the calculation of k_{app} leads to an absorption parameter (AP) defined as:

$$AP = \log\ (k_{app}) \quad (17)$$

The apparent kinetic constants (k_{app}) and the AP for all amine-based solvents tested in this work are presented in Tab. 3. These APs confirm the observations based on the absorption tests due to quite similar physicochemical properties (density, viscosity, CO_2 solubility, and diffusivity) of the CO_2-amine systems tested [25, 26].

4.2 Regeneration Results

The regeneration temperature temporal profiles during the regeneration tests achieved with the simple amine-based solvents (with a regeneration heating power of 600 W) are presented in Fig. 7. For all the solvents tested, the solution temperature increases during approximately the first 20 min and then stabi-

Table 3. Apparent kinetic constant (k_{app}) and absorption parameter (AP) of the amine-based solvents (at 298 K).

Solvents	($k_{2,exp}$) [$m^3kmol^{-1}s^{-1}$]	($k_{2,lit}$) [$m^3kmol^{-1}s^{-1}$]	(k_{app}) [s^{-1}]	AP
MDEA 30 wt-%	8.34	7.8 [31]	$2.16 \cdot 10$	1.33
AMP 30 wt-%	700	810 [32]	$2.26 \cdot 10^3$	3.35
MDEA 15 wt-% + MEA 15 wt-%	–	–	$2.16 \cdot 10^4$	4.33
MDEA 15 wt-% + PZEA 15 wt-%	–	–	$3.98 \cdot 10^4$	4.60
MEA 30 wt-%	8653	8400 [33]	$4.31 \cdot 10^4$	4.63
PZEA 30 wt-%	34 000	24 582 [34]	$7.96 \cdot 10^4$	4.90
PIP 15 wt-%	–	66 686 [35]	$1.17 \cdot 10^5$	5.07
MDEA 15 wt-% + PIP 15 wt-%	–	–	$1.17 \cdot 10^5$	5.07
AMP 15 wt-% + PIP 15 wt-%	–	–	$1.19 \cdot 10^5$	5.07
MDEA 15 wt-% + PZ 15 wt-%	–	–	$1.41 \cdot 10^5$	5.12
AMP 15 wt-% + PZ 15 wt-%	–	–	$1.43 \cdot 10^5$	5.12
PZ 15 wt-%	70 162	76 000 [36]	$1.51 \cdot 10^5$	5.18

lizes at the boiling point which is close to 375 K for all solvents except for PIP (369 K).

Concerning the CO_2 loading temporal profiles during regeneration of the simple amine-based solvents displayed in Fig. 8a, the clearly higher absorption capacities (α_{CO_2} ($t = 0$)) of PZEA 30 wt-% (1.59 mol CO_2/mol PZEA) and MDEA 30 wt-% (1.49 mol CO_2/mol MDEA) compared to MEA 30 wt-% (0.55 mol CO_2/mol MEA) and PZ 15 wt-% (0.76 mol CO_2/mol PZ) can be highlighted. AMP 30 wt-% and PIP 15 wt-% present intermediate values for this parameter (1.02 mol CO_2/mol AMP and 1.05 mol CO_2/mol PIP, respectively).

With these CO_2 loading temporal evolutions, the differences of regeneration behavior of the solvents can also be noted: at the end of the test, MDEA 30 wt-% is almost fully regenerated while other solvents and especially PZEA 30 wt-% still contain a significant CO_2 loading (~half of the initial loading). This observation can be confirmed by comparison of the pH temporal profiles (see Fig. 8b) to the pH value of the unloaded amine solutions (see Tab. 4).

The final pH of the MDEA 30 wt-% solution (11.21) is very close to the pH value of unloaded MDEA 30 wt-% (11.31) indicating an almost complete regeneration of the solution. On the contrary, the final pH of PZEA 30 wt-% solution (10.98) is still clearly different from the pH value of unloaded PZEA 30 wt-% (12.58) due to substantial CO_2 quantities remaining in solution. This observation can also be confirmed with other solvents. The different regeneration behaviors of the solvents are finally illustrated in Fig. 8c with the regeneration efficiency temporal profiles.

The almost complete regeneration of the tertiary amine MDEA 30 wt-% ($\eta_{regen}(7200\,s) \approx 100\,\%$) and the lower regeneration efficiency of PZEA 30 wt-% ($\eta_{regen}(7200\,s) = 50.5\,\%$) are confirmed. The better regeneration of PZ 15 wt-% ($\eta_{regen}(7200\,s) = 88.5\,\%$) and AMP 30 wt-% ($\eta_{regen}(7200\,s) = 86.4\,\%$) compared to MEA 30 wt-% ($\eta_{regen}(7200\,s) = 62.9\,\%$) and PIP 15 wt-% ($\eta_{regen}(7200\,s) = 57.8\,\%$) can also be noticed.

Regarding the regeneration results relative to the blended amine solutions, Figs. 9a–c illustrate the temporal profiles of CO_2 loading, pH, and regeneration efficiency of the solutions (with a similar heating power fixed at 600 W). The highest absorption capacities (α_{CO_2} ($t = 0$) in Fig. 9a) are obtained with AMP 15 wt-% solutions blended with PZ 15 wt-% or PIP 15 wt-%, and the lowest with MDEA 30 wt-% + MEA 15 wt-% solutions. As in the case of simple amine solutions, the pH temporal profiles (Fig. 9b) are coherent with the CO_2 loading profiles, the final pH of the solutions being closer to the pH value of the unloaded solution (Tab. 4) when the CO_2 content remaining in solution is lower.

Table 4. pH of unloaded amine solutions.

Solvents	pH of unloaded solutions
MDEA 30 wt-%	11.31
MEA 30 wt-%	12.30
PZEA 30 wt-%	12.58
PZ 15 wt-%	12.19
PIP 15 wt-%	12.48
AMP 30 wt-%	12.74
MDEA 15 wt-% + MEA 15 wt-%	12.28
MDEA 15 wt-% + PZEA 15 wt-%	12.15
MDEA 15 wt-% + PZ 15 wt-%	12.38
MDEA 15 wt-% + PIP 15 wt-%	12.85
AMP 15 wt-% + PZ 15 wt-%	12.50
AMP 15 wt-% + PIP 15 wt-%	12.91

In terms of regeneration efficiency (Fig. 9c), even if PZEA was the worst simple amine solution to regenerate, the blend of MDEA 15 wt-% and PZEA 15 wt-% has the better final regeneration efficiency ($\eta_{regen}(7200\,s) = 97.8\,\%$) among the amine blends. The other blends exhibit lower final regeneration efficiencies as, e.g., the MDEA 15 wt-% + MEA 15 wt-% blend ($\eta_{regen}(7200\,s) = 73.3\,\%$), MDEA 15 wt-% + PZ 15 wt-% blend ($\eta_{regen}(7200\,s) = 64.5\,\%$), and AMP 15 wt-% + PZ 15 wt-% blend ($\eta_{regen}(7200\,s) = 64.4\,\%$). The clearly lower final regeneration efficiencies of the MDEA 15 wt-% and AMP 15 wt-% solutions blended with PIP 15 wt-% ($\eta_{regen}7200\,s) = 46\,\%$ and $52.3\,\%$, respectively) are illustrated in Fig. 9c. The regeneration efficiencies after 7200 s (in hatched lines) and after 1200 s (in black) of the simple and blended amine solutions are compared in Fig. 10.

Differences can be observed between $\eta_{regen}(7200\,s)$ and $\eta_{regen}(1200\,s)$ solvent rankings. Actually, $\eta_{regen}(7200\,s)$ is rather an indicator of the solvent desorption capacity while $\eta_{regen}(1200\,s)$ provides more information about its regeneration kinetics. Given the fact that in the industrial CO_2 capture process the solvents are never completely regenerated according to an

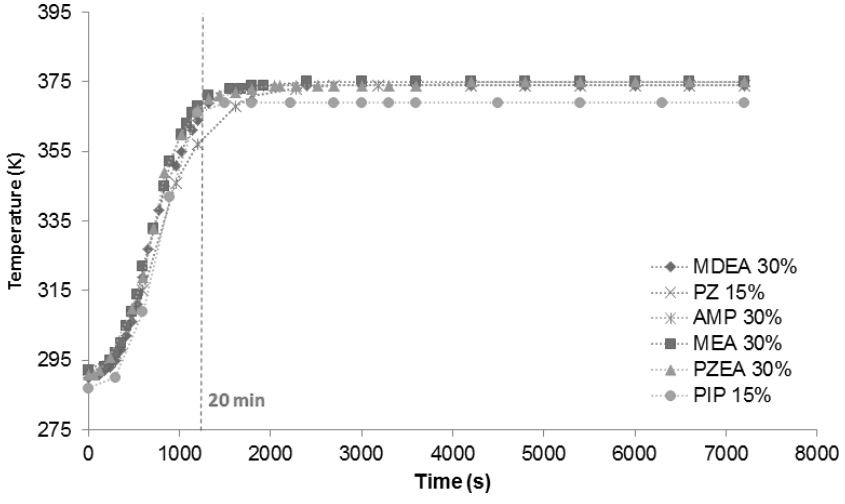

Figure 7. Regeneration temperature temporal profiles during the regeneration tests of the simple amine-based solvents.

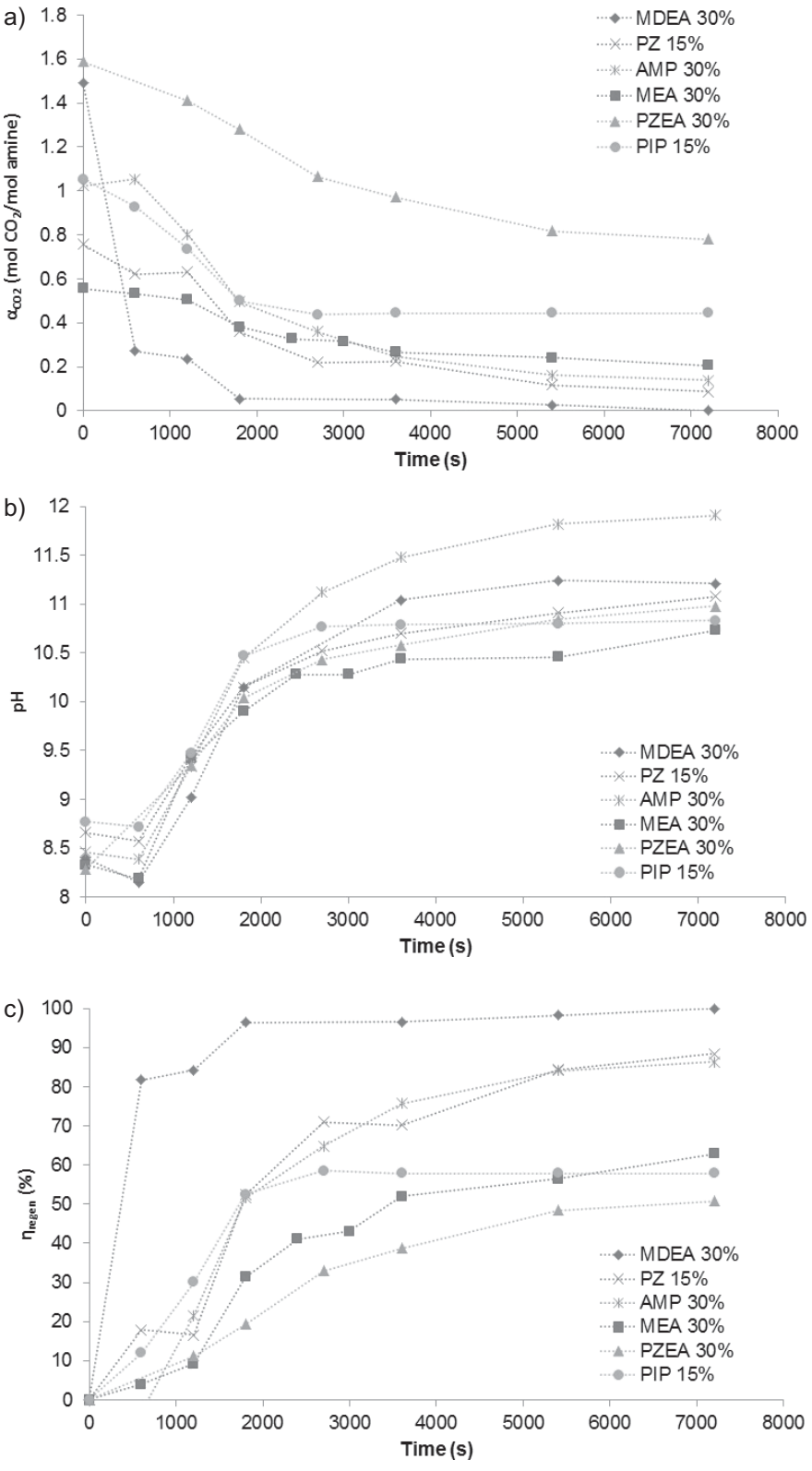

Figure 8. CO_2 loading (a), pH (b), and regeneration efficiency (c) temporal profiles during the regeneration tests of the simple amine-based solvents.

energetic optimum [38], the kinetic aspect needs to be taken into account in the definition of a parameter characterizing regeneration.

As already developed by other authors such as [39], the desorption rate (r_{des}) of each solvent is defined as in the initial slope of the CO_2 concentration temporal profile:

$$r_{des} = \frac{dC_{CO_2}}{dt}(t = 0) \quad (18)$$

By dividing the desorption rate by the initial CO_2 concentration (C_{CO_2} (t = 0)), the desorption kinetic constant (k_{des}) is obtained:

$$k_{des} = \frac{r_{des}}{C_{CO_2}(t = 0)} \quad (19)$$

As assumed in [39], the regeneration energy of a solvent could be inversely proportional to k_{des} defined at $t = 0$ because the regeneration behavior of the solution at the beginning of the experiment is rather representative for the industrial conditions of the process where rich solutions (with a quite important CO_2 loading) are regenerated.

The regeneration parameter (RP) of the solvent is defined as being proportional to the regeneration energy:

$$RP = \log\left(\frac{1}{k_{des}}\right) \quad (20)$$

The desorption rate, desorption kinetic constant, and regeneration parameter of all the amine-based solvents tested are listed in Tab. 5. Obviously, the RPs have similar orders of magnitude as the regeneration energy (see, e.g., [40] with regeneration energies of MEA, MDEA, and MEA-MDEA varying between 1.5 and 4 GJ/t_{CO_2}, depending on CO_2 loading conditions).

A tertiary amine such as MDEA 30 wt-%, which is known for requiring low regeneration energy, has a low RP (2.87) in contrast to a primary amine such as MEA 30 wt-% (4.11). Comparing the other simple amine solutions, PZ 15 wt-%, PIP 15 wt-%, and AMP 30 wt-% with RPs of to 3.53, 3.54, and 3.64 exhibit lower RPs than PZEA 30 wt-% (4.03) which would indicate a lower regeneration energy require-

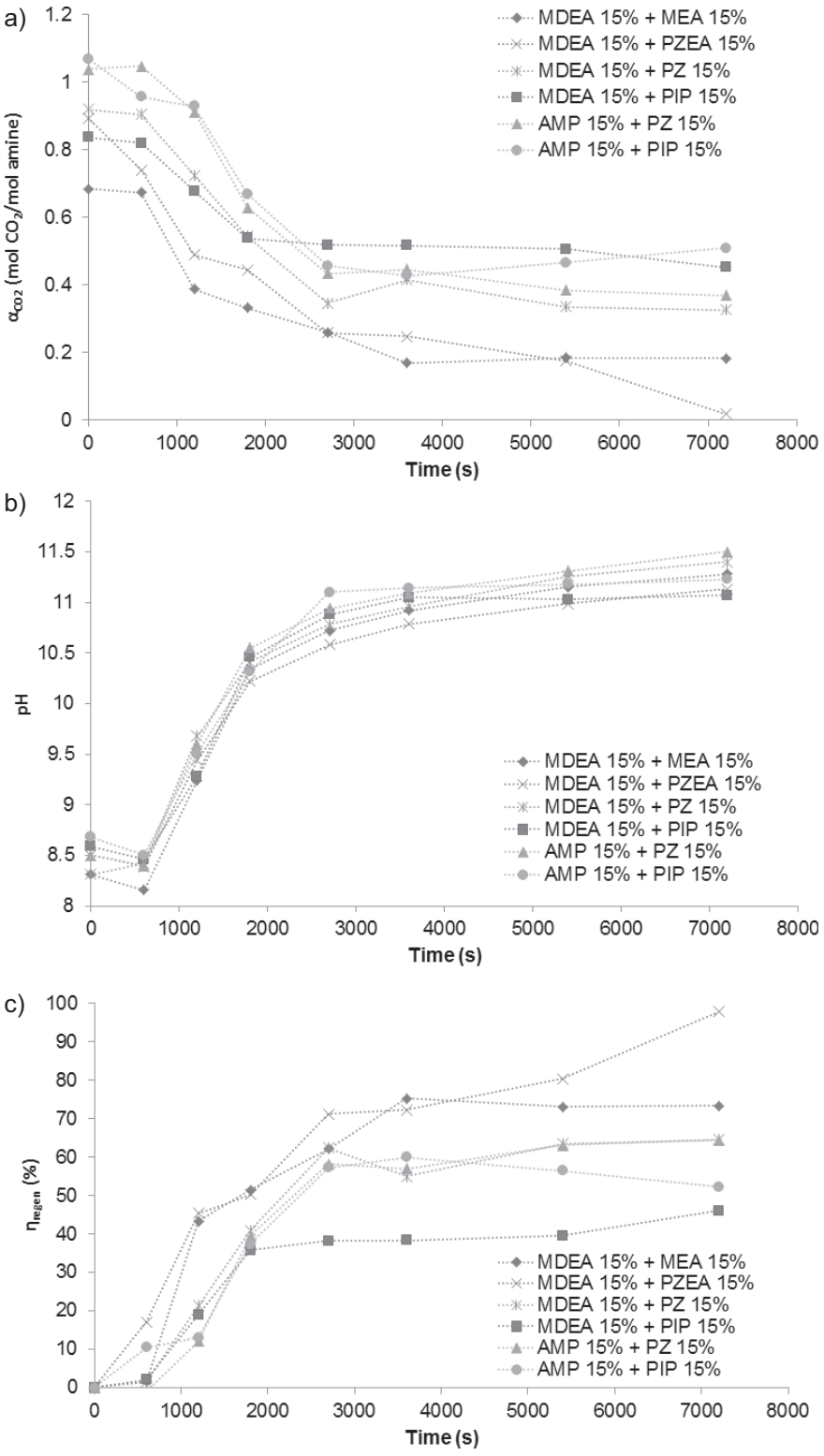

Figure 9. CO_2 loading (a), pH (b), and regeneration efficiency (c) temporal profiles during the regeneration tests of the blended amine-based solvents.

ment. Regarding the blends of amines, MDEA 15 wt-% + PZEA 15 wt-% and MDEA 15 wt-% + MEA 15 wt-% have lower RPs (3.42 and 3.44) than all the other blends whose RP values vary between 3.64 (MDEA 15 wt-% + PZ 15 wt-%) and 3.70 (MDEA 15 wt-% + PIP 15 wt-%).

4.3 Global Comparison of Solvents

A potentially interesting solvent for the CO_2 capture process must simultaneously present high absorption performances (high AP) and a regeneration energy requirement as low as possible (low RP), presented as "Target" in Fig. 11.

Fig. 11 illustrates that compared to MEA, cyclical amines and activated solutions of MDEA and AMP with PZ and PIP present a relatively high AP simultaneously to a lower RP. To achieve more precisely a quantitative comparison of the absorption-regeneration performances of all the solvents tested, a lumped global solvent parameter (GSP) can be defined as a numerical indicator which has to be maximized:

$$\mathrm{GSP} = \frac{\mathrm{AP}}{\mathrm{RP}} \tag{21}$$

The GSP values calculated for of all the amine(s)-based solvents tested are presented in the legend of Fig. 11.

The good potential of cyclical amines (PIP 15 wt-% and PZ 15 wt-%) is confirmed by their high GSP values (1.43 and 1.47) compared to other simple amine solutions (GSP <1.25) with a particularly low value for MDEA 30 wt-% (0.46) due to its very bad absorption performances. Regarding the different activated solutions of MDEA and AMP, the best GSP results are obtained for PZ as activator (1.41), the value being slightly lower for PIP and PZEA (1.35–1.38). The value for the MDEA 15 wt-% + MEA 15 wt-% mixture (1.26) is clearly lower than for other amine blends.

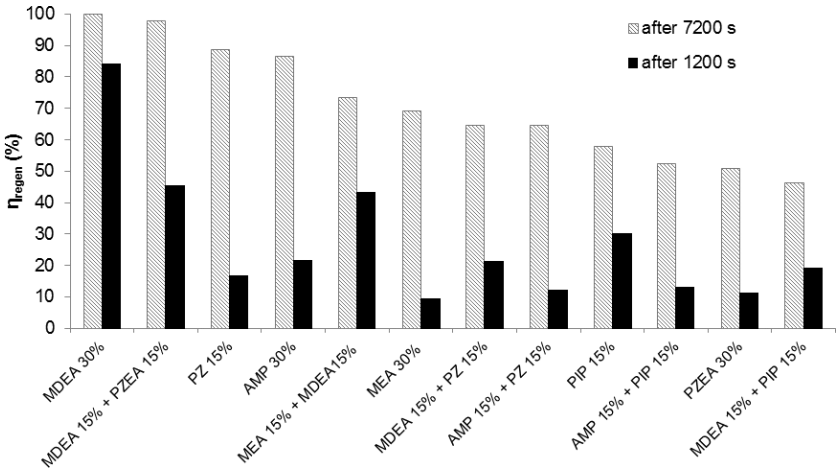

Figure 10. Regeneration efficiencies (after 1200 and 7200 s) for all tested amine-based solvents.

Table 5. Desorption rate (r_{des}), desorption kinetic parameter (k_{des}), and regeneration parameter (RP) of the amine-based solvents evaluated during the regeneration tests.

Solvents	r_{des} [kmol·m^{-3}s^{-1}]	k_{des} [s^{-1}]	RP
MDEA 30 wt-%	$5.04 \cdot 10^{-3}$	$1.36 \cdot 10^{-3}$	2.87
MDEA 15 wt-% + PZEA 15 wt-%	$8.67 \cdot 10^{-4}$	$3.77 \cdot 10^{-4}$	3.42
MDEA 15 wt-% + MEA 15 wt-%	$8.75 \cdot 10^{-4}$	$3.61 \cdot 10^{-4}$	3.44
PZ 15 wt-%	$4.47 \cdot 10^{-4}$	$2.97 \cdot 10^{-4}$	3.53
PIP 15 wt-%	$5.16 \cdot 10^{-4}$	$2.92 \cdot 10^{-4}$	3.54
AMP 30 wt-%	$5.81 \cdot 10^{-4}$	$2.23 \cdot 10^{-4}$	3.64
MDEA 15 wt-% + PZ 15 wt-%	$6.13 \cdot 10^{-4}$	$2.27 \cdot 10^{-4}$	3.64
AMP 15 wt-% + PZ 15 wt-%	$6.93 \cdot 10^{-4}$	$2.19 \cdot 10^{-4}$	3.66
AMP 15 wt-% + PIP 15 wt-%	$7.26 \cdot 10^{-4}$	$2.07 \cdot 10^{-4}$	3.68
MDEA 15 wt-% + PIP 15 wt-%	$5.60 \cdot 10^{-4}$	$1.99 \cdot 10^{-4}$	3.70
PZEA 30 wt-%	$3.18 \cdot 10^{-4}$	$9.32 \cdot 10^{-5}$	4.03
MEA 30 wt-%	$1.92 \cdot 10^{-4}$	$7.69 \cdot 10^{-5}$	4.11

5 Conclusions and Perspectives

In order to implement the CO_2 capture process by chemical absorption into aqueous amine(s)-based solvents, separate absorption and regeneration tests were performed for deduction of relevant parameters characterizing and comparing the absorption-regeneration performances of different types of solvents and their blends. In a first step, absorption test runs achieved at 298 K and atmospheric pressure in a laboratory cable-bundle scrubber allowed to compare the CO_2 absorption efficiencies of several amine-based solvents. Applying a modeling method based on the two-film theory which is suited for absorption accompanied by chemical reaction, apparent kinetic constants and absorption parameters were deduced from absorption test runs. In a second step, a regeneration device has been used in order to compare the regeneration efficiencies of different types of solvents (simple and blended) at their boiling temperature (around 375 K) and with a constant heating power of 600 W. Desorption kinetic constants and regeneration parameters were obtained from these experiments.

Finally, a GSP can be defined as an interesting indicator for the quantitative comparison of absorption-regeneration performances of all the solvents tested. The good potential of cyclical amines (PIP 15 wt-% and PZ 15 wt-%) was confirmed with their high GSP values compared to the other simple amine solutions with a particularly low GSP value for MDEA 30 wt-% because of its poor absorption performances despite its good regeneration performances. Regarding the different activated solutions of MDEA and AMP, the best results were obtained with the addition of PZ as activator.

Such laboratory experimental setup and methodology can be suitable to achieve similar runs in order to characterize other solutions of amines or solvents, or mixtures of amines involving more complex reaction mechanisms. It is planned to compare the present solvents ranking with another one based on GSP values that are deduced from coupled absorption-regeneration tests achieved with a micro-pilot unit. This study is still in progress.

Acknowledgment

L. Dubois gratefully acknowledges research support from the Chemical Engineering Department of the Faculty of Engineering (University of Mons) and the Holcim Company during his thesis.

The authors have declared no conflict of interest.

Symbols used

a	[m^{-1}]	specific interfacial area
A	[–]	absorption efficiency
C_{amine}	[kmol m^{-3}]	total amine concentration of the solvent
C_{CO_2}	[kmol m^{-3}]	CO_2 concentration in the liquid phase
$D_{CO_2/Amine}$	[m^{2}s^{-1}]	CO_2 diffusion coefficient in the amine solution
dh	[m]	height of the increment volume
E	[–]	enhancement factor

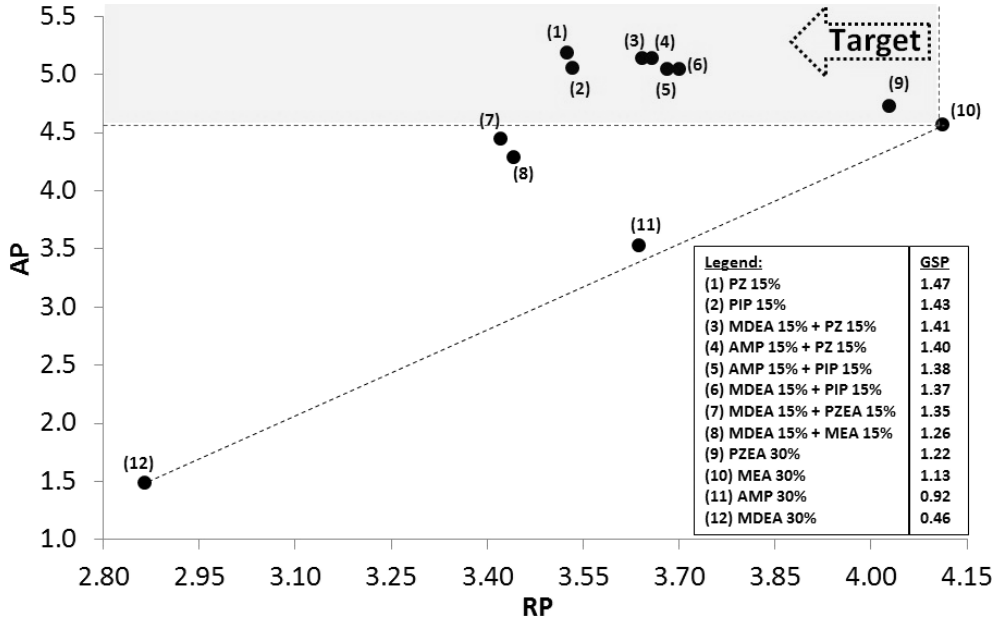

Figure 11. Combined comparison of the absorption parameters (AP) and regeneration parameters (RP) of all amine-based solvents.

E_{regen}	[GJ $t_{CO_2}^{-1}$]	regeneration energy of the solvent
G	[$m^3 s^{-1}$]	volumetric gas flow rate
$H_{CO_2/Amine}$	[Pa $m^3 kmol^{-1}$]	CO_2 Henry's coefficient for amine solutions
$\Delta H_{reaction}$	[GJ $t_{CO_2}^{-1}$]	reaction heat of the CO_2-amine reaction
$\Delta H_{sensible}$	[GJ $t_{CO_2}^{-1}$]	sensible heat to reach the regeneration temperature
$\Delta H_{vaporization}$	[GJ $t_{CO_2}^{-1}$]	vaporization heat of the solvent
Ha	[–]	Hatta number
k_G	[kmol $s^{-1} m^{-2} Pa^{-1}$]	gas-phase mass transfer coefficient
k_L	[m s^{-1}]	liquid-phase mass transfer coefficient
k_2	[$m^3 kmol^{-1} s^{-1}$]	second-order kinetic constant
k_{app}	[s^{-1}]	apparent kinetic constant
k_{des}	[s^{-1}]	desorption kinetic constant
n	[–]	stoichiometry of the global CO_2/amine reaction
P	[W]	heating power
p_{CO_2}	[Pa]	partial pressure of CO_2
R_{CO_2}	[kmol $m^{-2} s^{-1}$]	CO_2 absorption flux
r_{des}	[kmol $m^{-3} s^{-1}$]	desorption rate
S	[m^2]	section of the contactor
T	[K]	temperature
y_{CO_2}	[vol.-%]	CO_2 volume percentage of the gas

Greek symbols

α_{CO_2}	[mol mol^{-1}]	CO_2 loading of the liquid
$\Delta\alpha_{CO_2}$	[mol mol^{-1}]	CO_2 cycling capacity
η_{regen}	[–]	regeneration efficiency

Subscripts

exp	relative to the experiment
i	interface
j	number of absorption experimental points
I	inlet of the incremental volume
in	inlet of the contactor
lit	relative to literature values
O	outlet of the incremental volume
out	outlet of the contactor
sim	relative to the simulation
x	number of amines in a mixture

References

[1] M. Anheden, J. Yan, G. De Smedt, *Oil Gas Sci. Technol.* **2005**, *60 (3)*, 485.
[2] L. I. Eide, D. W. Bailey, *Oil Gas Sci. Technol.* **2005**, *60 (3)*, 475.
[3] D. W. Bailey, P. H. M. Feron, *Oil Gas Sci. Technol.* **2005**, *60 (3)*, 461.
[4] H. Lepaumier, D. Picq, P. L. Carrette, *Energy Procedia* **2009**, *1*, 893.
[5] I. Eide-Haugmo, H. Lepaumier, A. Einbu, K. Vernstad, E. F. da Silva, H. F. Svendsen, *Energy Procedia* **2011**, *4*, 1631.
[6] J. Kittel, R. Idem, D. Gelowitz, P. Tontiwachwuthikul, G. Parrain, A. Bonneau, *Energy Procedia* **2009**, *1*, 791.
[7] M. Nainar, A. Veawab, *Energy Procedia* **2009**, *1*, 231.
[8] I. Eide-Haugmo, O. G. Brakstad, K. A. Hoff, K. R. Sørheim, E. F. da Silva, H. F. Svendsen, *Energy Procedia* **2009**, *1*, 1297.
[9] T. Nguyen, M. Hilliard, G. T. Rochelle, *Int. J. Greenhouse Gas Control* **2010**, *4 (5)*, 707.
[10] A. N. M. Peeters, A. P. C. Faaij, W. C. Turkenburg, *Int. J. Greenhouse Gas Control* **2007**, *1 (4)*, 396.

[11] L. Raynal, P. Font, T. Janeiro, Y. Haroun, P.-A. Bouillon, *Distillation Absorption Proceedings* (Eds: A. B. de Haan, H. Kooijman, A. Gorak), Eindhoven University of Technology, Eindhoven **2010**, 121.
[12] P. D. Vaidya, E. Y. Kenig, *Chem. Eng. Technol.* **2007**, *30 (11)*, 1467.
[13] P. M. M. Blauwhoff, G. F. Versteeg, W. P. M. Van Swaaij, *Chem. Eng. Sci.* **1984**, *39 (2)*, 207.
[14] M. Caplow, *J. Am. Chem. Soc.* **1968**, *90 (24)*, 6795.
[15] P. D. Danckwerts, *Chem. Eng. Sci.* **1979**, *34 (4)*, 443.
[16] A. Veawab, A. Aroonwilas, *IJGGC* **2007**, *1 (3)*, 143.
[17] I. Kim, H. F. Svendsen, *Int. J. Greenhouse Gas Control* **2011**, *5 (3)*, 390.
[18] F. Bougie, M. C. Iliuta, *Chem. Eng. Sci.* **2009**, *64*, 153.
[19] G. Sartori, D. W. Savage, *Ind. Eng. Chem. Fundam.* **1983**, *22*, 239.
[20] P. W. J. Derks, *Ph. D. Thesis*, Twente University of Technology **2006**.
[21] S. Bishnoi, *Ph. D. Thesis*, University of Texas **2000**.
[22] F. A. Chowdhury, H. Okabe, H. Yamada, Y. Masami, Y. Fujioka, *Energy Procedia* **2011**, *4*, 201.
[23] K. Goto, F. A. Chowdhury, H. Okabe, S. Shimizu, Y. Fujioka, *Energy Procedia* **2011**, *4*, 253.
[24] J. Oexmann, A. Kather, *Int. J. Greenhouse Gas Control* **2010**, *4*, 36.
[25] L. Dubois, D. Thomas, *Chem. Eng. Technol.* **2009**, *32 (5)*, 710.
[26] L. Dubois, P. Kahasha Mbasha, D. Thomas, *Chem. Eng. Technol.* **2010**, *33 (3)*, 461.
[27] F. Bougie, M. C. Iliuta, *Chem. Eng. Sci.* **2010**, *65*, 4746.
[28] P. Zhang, Y. Shi, J. Wei, W. Zhao, Q. Ye, *J. Environ. Sci.* **2008**, *20*, 39.
[29] C. Roizard et al., *Tech. Ing.*, *Traité Génie des Procédés* **1997**, Ref. J 1 079.
[30] L. Dubois, D. Thomas, *Energy Procedia* **2011**, *4*, 1353.
[31] J. Benitez-Garcia, G. Ruiz-Ibanez, H. Al-Ghawas, O. C. Sandall, *Chem. Eng. Sci.* **1991**, *46 (11)*, 2927.
[32] S. Xu, Y. W. Wang, F. D. Otto, A. E. Mather, *Chem. Eng. Sci.* **1996**, *51*, 841.
[33] E. Sada, H. Kumazawa, M. A. Butt, *Can. J. Chem. Eng.* **1976**, *54 (5)*, 421.
[34] S. Paul, A. K. Ghoshal, B. Mandal, *Chem. Eng. Sci.* **2009**, *64*, 1618.
[35] G. F. Versteeg, L. A. J. van Dijck, W. P. M. van Swaaij, *Chem. Eng. Commun.* **1996**, *144 (1)*, 113.
[36] P. W. J. Derks, T. Kleingeld, C. van Aken, J. A. Hogendoorn, G. F. Versteeg, *Chem. Eng. Sci.* **2006**, *61 (20)*, 6837.
[37] G.-W. Xu, C.-F. Zhang, S.-J. Qin, Y.-W. Wang, *Ind. Eng. Chem. Res.* **1992**, *31 (3)*, 921.
[38] P. Alix, P. Broutin, T. Burkhardt, *Procédique* **2007**, *42*, 6.
[39] P. Singh, G. F. Versteeg, *Process Saf. Environ. Prot.* **2008**, *86*, 347.
[40] M. Wilson, P. Tontiwachwuthikul, A. Chakma, R. Idem, A. Veawab, A. Aroonwilas, *Greenhouse Gas Control Technol.* **2005**, *7*, 55.

